ELSEVIER

Polymer Vol. 37 No. 14, pp. 3087–3092, 1996

0032-3861/96/$15.00+0.00

Reaction-induced phase separation in poly(butylene terephthalate)–epoxy systems: 2. Morphologies generated and resulting properties

P. A. Oyanguren, P. M. Frontini and R. J. J. Williams*
Institute of Materials Science and Technology (INTEMA), University of Mar del Plata and National Research Council (CONICET), J. B. Justo 4302, (7600) Mar del Plata, Argentina

and G. Vigier
GEMPPM, Bât. 502, URA CNRS no. 431, Institut National des Sciences Appliquées de Lyon, 20 Av. A. Einstein, 69621 Villeurbanne Cedex, France

and J. P. Pascault
Laboratoire des Matériaux Macromoléculaires, Bât. 403, URA CNRS no. 507, Institut National des Sciences Appliquées de Lyon, 20 Av. A. Einstein, 69621 Villeurbanne Cedex, France
(Received 9 October 1995)

Poly(butylene terephthalate) (PBT) was used as a semicrystalline modifier of epoxy–aromatic diamine formulations in concentrations ranging from about 3 wt% to 8 wt%. The epoxy monomer was based on diglycidylether of bisphenol A (DGEBA) and the diamines were either 4,4′-methylenebis [3-chloro 2,6-diethylaniline] (MCDEA) and 4,4′-diaminodiphenylsulfone (DDS). Using conversion–temperature transformation diagrams developed in part 1, thermal cycles were selected to generate different morphologies. In the case of PBT–DGEBA–DDS systems, phase separation in the course of reaction led to a random dispersion of spherical particles (sizes in the range of 1 μm), rich in PBT. Small and wide angle X-ray scattering, carried out *in situ*, during cure, revealed that the dispersion of spherical particles was produced by a nucleation-growth mechanism and that crystallization took place after phase separation. A completely different morphology, characterized by a distribution of large and irregular semicrystalline particles, was produced by crystallization before reaction. However, both types of morphologies introduced a small increase in the critical stress intensity factor. The main toughening mechanism was crack bridging produced by highly drawn thermoplastic particles. On the other hand, PBT–DGEBA–MCDEA formulations were cured at temperatures high enough to avoid crystallization of PBT during reaction. In this case, the PBT remaining dissolved in the matrix did not introduce any toughening effect. Copyright © 1996 Elsevier Science Ltd.

(Keywords: poly(butylene terephthalate); epoxy; modified-epoxies)

INTRODUCTION

In part 1 of the series[1], phase separation of poly(butylene terephthalate) (PBT) from an epoxy–amine matrix, in the course of reaction, was analysed in the frame of conversion–temperature transformation diagrams (CTT). It was established that for a diglycidyl-ether of bisphenol A (DGEBA)–4,4′-methylenebis 3-chloro 2,6-diethylaniline (MCDEA) system, PBT could be kept in solution when the reaction was carried out at temperatures high enough to avoid PBT crystallization. However, for DGEBA–4,4′-diaminodiphenylsulfone (DDS) systems, PBT was phase separated in the course of reaction even when operating at temperatures higher than the melting temperature of pure PBT.

Therefore, morphologies generated and associated thermal and mechanical properties, may be varied by selecting different cure trajectories in the respective CTT diagrams[1]. An analysis of several possibilities will be presented in this part of the series.

EXPERIMENTAL

Materials and sample preparation

Chemical structures and properties of the epoxy monomer (DGEBA), aromatic diamines (MCDEA and DDS) and the modifier (PBT), were described in the first part[1]. PBT was dissolved in previously degassed DGEBA by heating the mixture at $T = 230$°C during 30 min. Then, the solution was cooled to 135°C, in the case of DDS, or 90°C, in the case of MCDEA, and a

* To whom correspondence should be addressed

stoichiometric amount of the aromatic diamine was added by heating during about 5 min. During the cooling period, crystallization of PBT produced a stable dispersion of crystals with sizes in the 10 μm range. When the PBT-modified epoxy–amine dispersion was heated again above the melting temperature of PBT, a homogeneous solution was obtained. The high viscosity of PBT–epoxy–amine mixtures made it not possible to introduce more than 7–8% mass fraction of PBT for casting purposes. The following PBT mass fractions were selected: 3.3% for DGEBA–MCDEA mixtures and 3.75% or 7.5% for DGEBA–DDS formulations.

Plates for subsequent mechanical characterization (flexural, compression and fracture tests), were obtained by casting the mixture into a mould consisting of two glass plaques coated with siliconized paper and spaced by a 6 mm diameter rubber cord. Cure was carried out in an oven following a predetermined thermal cycle.

Small and wide angle X-ray scattering

Small angle X-ray scattering (SAXS) was performed with a set-up including a rotating anode X-ray generator with a copper target and nickel filter ($\lambda = 1.54$ Å), a point collimation produced mainly by two orthogonal mirrors and a line position sensitive proportional counter connected to a computer. The intensity (I) in the angular range $0.085° < 2\theta < 0.65°$ (2θ = scattering angle in radians), was obtained as a function of the scattering vector

$$q = (4\pi/\lambda)\sin\theta \tag{1}$$

Samples were heated *in situ* from room temperature up to the selected cure temperature and held at this value ($\Delta T = \pm 1°C$). Time zero was taken from the attainment of the constant temperature level. The domain size detectable by the SAXS set-up was comprised from about 30 Å to 500 Å, as discussed elsewhere[2].

Wide angle X-ray scattering (WAXS) was performed with the same apparatus used for SAXS except that the scattering angle was varied in the range, $2\theta = 10°$–$25°$.

Mechanical characterization

Dynamic mechanical spectra of fully cured materials were obtained with a Perkin-Elmer DMA-7 system, operating at 1 Hz in the three-point-bending mode.

Mechanical tests were performed at 20°C using a Shimadzu Autograph SC-500 universal testing machine. Samples for mechanical characterization were machined from the plates cured in the oven. Flexure moduli were determined using sample dimensions recommended by ASTM standards. Uniaxial compression tests were performed at a constant crosshead speed of 0.5 mm min^{-1} on specimens with dimensions of about 5 × 5 × 12 mm. The strain (ϵ) was determined from the crosshead displacement. The load (P) was converted into true stress (σ) using the initial cross-sectional area A_0 in the equation:

$$\sigma = P(1 - \epsilon)/A_0 \tag{2}$$

Yield stress (σ_y) was taken at the maximum of the stress-strain curve.

Fracture tests were performed at a crosshead speed of 10 mm min^{-1}. Single-edge notched specimens in three-point bending mode (SENB) were used. Dimensions were the following: thickness (B) = 6 mm, width (W) = 12 mm, and span-to-length (L) = 48 mm. Sharp initial cracks of length (a) were obtained by first machining the notch and then generating a natural crack by tapping on a new razor blade placed in the notch of the pre-compressed specimen.

The critical stress intensity factor, K_{Ic}, was calculated from

$$K_{Ic} = \sigma_c(\pi a)^{1/2} f(a/W) \tag{3}$$

where $\sigma_c = 3P_cL/(2BW^2)$ is the critical stress for crack propagation and $f(a/W)$ is a calibration factor given by

$$f(a/W) = 1.09 - 1.735(a/W) + 8.2(a/W)^2 - 14.18(a/W)^3 + 14.57(a/W)^4 \tag{4}$$

K_{Ic} was determined from the slope of a plot of $\sigma_c(\pi a)^{1/2}$ *versus* $1/f(a/W)$, obtained from at least ten different experimental tests. The length of the initial crack (a) was obtained from the surface of the broken samples using a profile projector (×10), averaging the results in five points as suggested by ASTM E399 standard.

Scanning electron microscopy

Fracture surfaces were observed by scanning electron microscopy (SEM) (Jeol JSM 35 CF), after coating with a fine gold layer. Micrographs were magnified and regions containing about 250 particles of dispersed phase were analysed. An image-processing program was used to find the average diameter of dispersed-phase particles,

$$\bar{D} = \sum n_i D_i / \sum n_i \tag{5}$$

and the volume fraction of dispersed phase,

$$V_D = \pi \sum n_i D_i^2 / (4A_T) \tag{6}$$

where A_T is the area of the micrograph region under analysis. Equation (6) assumes that area and volume fractions of dispersed-phase particles are the same.

RESULTS AND DISCUSSION

PBT–DGEBA–DDS systems

Figure 1 shows melting and cloud-point curves in a

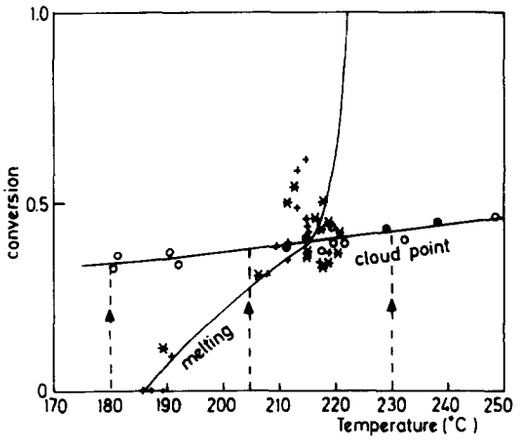

Figure 1 CTT diagram for PBT–DGEBA–DDS systems showing melting (T_m) and cloud-point curves (T_{cp}). 3.75 wt% PBT: *, T_m; O, T_{cp}; 7.5 wt% PBT: +, T_m; ●, T_{cp}

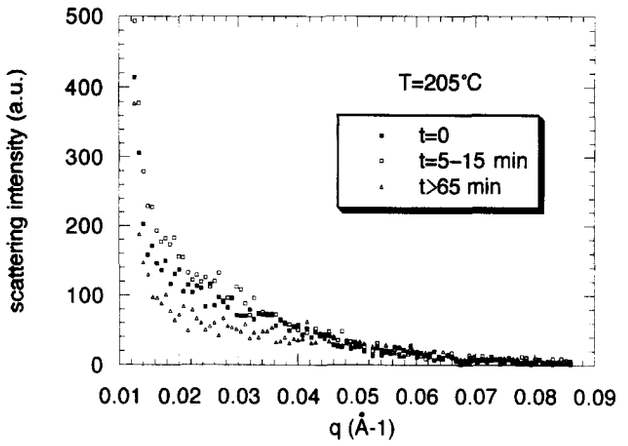

Figure 2 SAXS intensity (arbitrary units) as a function of the scattering vector q ($Å^{-1}$), for different cure times at 205°C (PBT–DGEBA–DDS system containing 7.5 wt% PBT)

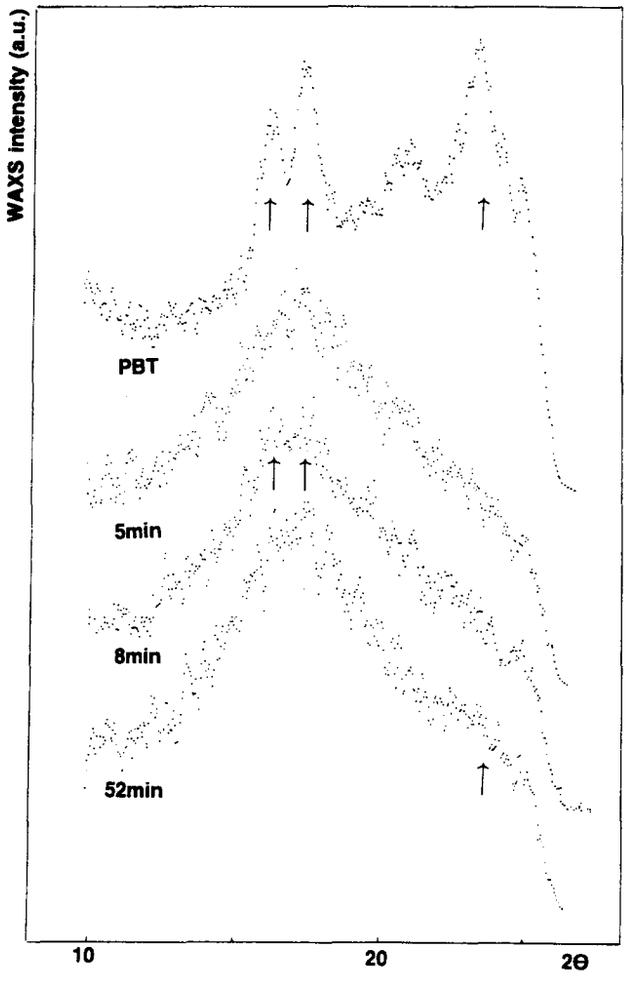

Figure 3 WAXS intensity (arbitrary units) as a function of the scattering angle, for different cure times at 205°C (PBT–DGEBA–DDS system containing 7.5 wt% PBT). The WAXS pattern of pure PBT is also shown for comparison purposes

CTT diagram. Three trajectories are indicated at different reaction temperatures T_i. At $T_i = 180°C$, PBT crystals are present from the beginning of reaction; at $T_i = 230°C$, an amorphous phase rich in PBT is phase separated in the course of reaction (crystallization of PBT domains takes place during the cooling step after full cure of the epoxy–amine matrix). At $T_i = 205°C$, there is a competition between crystallization, that may begin to occur when entering the region bounded by the melting curve, and phase separation of an amorphous phase at the cloud-point curve, followed by PBT crystallization in dispersed domains. To elucidate the phase separation mechanism in this temperature region, *in situ* SAXS and WAXS measurements were performed.

Figure 2 shows SAXS intensity as a function of the scattering vector, for a PBT–DGEBA–DDS system

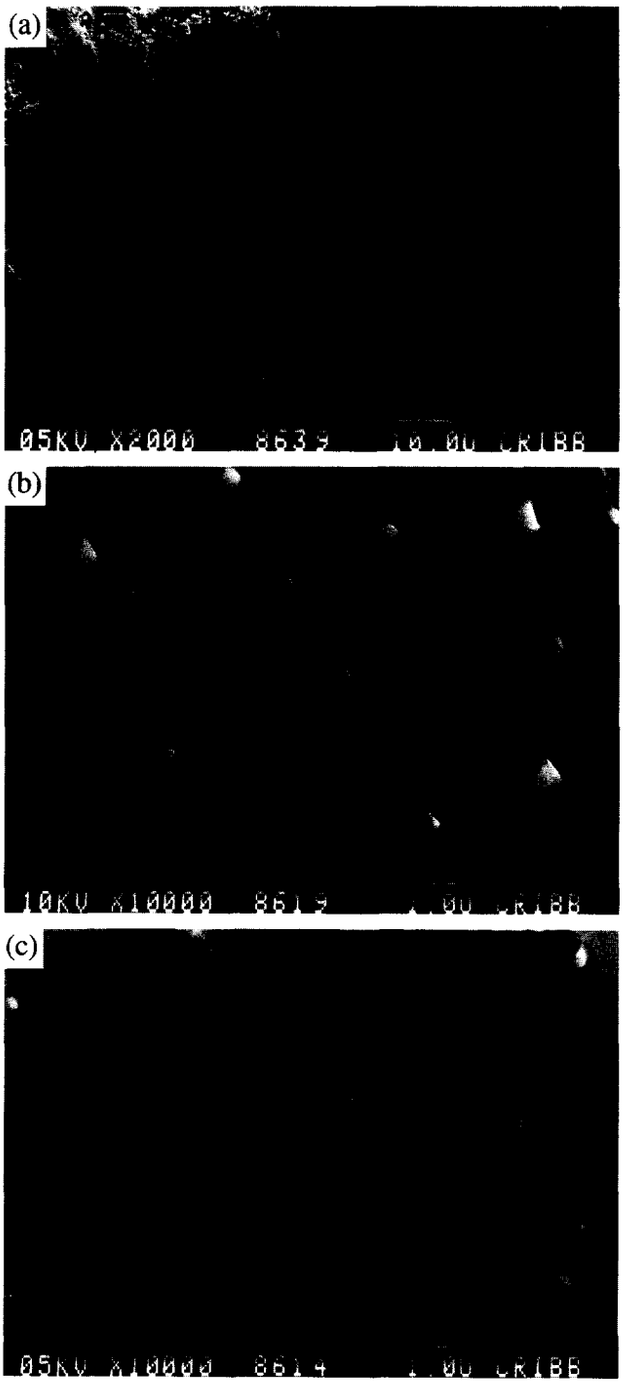

Figure 4 SEM micrographs of fracture surfaces of PBT–DGEBA–DDS materials: (a) 3.75 wt% PBT, cured 2 h at 180°C and 2 h at 230°C; (b) 3.75 wt% PBT, cured 15 min at 230°C and 3.5 h at 200°C; (c) 7.5 wt% PBT, cured 15 min at 230°C and 3.5 h at 200°C

containing 7.5 wt% PBT, cured at $T_i = 205°C$ in the SAXS set-up. At $t = 5$ min, an increase in SAXS intensity, assigned to the appearance of a second phase, is observed. Kinetic runs carried out at $T_i = 200°C$, showed a conversion located in the 0.30–0.35 range, after a 5 min-cure[1]. Although no strict comparison with the conversion attained in the SAXS device may be made (due to the possible advance of reaction during the heating period and the slightly different temperature levels (205°C and 200°C), a time scale of 5 min is reasonable to get the cloud-point conversion at $T_i = 205°C$ (*Figure 1*).

The continuous decrease of I with q (*Figure 2*), is characteristic of a random distribution of dispersed phase particles (there is no characteristic length where intensity exhibits a maximum value). This is typical of phase separation produced by a nucleation-growth mechanism, i.e. as opposed to a spinodal demixing mechanism. As shown in *Figure 2*, after 15 min reaction a decrease in the scattered intensity is observed. This is possibly due to the size increase of dispersed phase particles that sets them outside the SAXS-sensitivity window. At long times, the scattered intensity is lower than the initial value.

Figure 3 shows WAXS intensity as a function of the scattering angle, obtained under exactly the same conditions as those used for SAXS. The scattering pattern produced by pure PBT is also shown for comparison purposes. The appearance of diffraction peaks (indicated by arrows) after 8 min cure at $T_i = 205°C$, indicates a partial crystallization of PBT in dispersed domains.

Simultaneous analysis of both SAXS and WAXS results suggests that, at $T_i = 205°C$, PBT gets phase separated when the cloud-point curve is reached and soon after crystallization begins to take place inside dispersed domains.

Figure 4 shows SEM micrographs of fracture surfaces of materials containing 3.75 and 7.5 wt% PBT, cured using different thermal cycles. The material obtained by curing at $T_i = 180°C$ (*Figure 4a*) shows the presence of a dispersed semicrystalline phase initially present before reaction. Structures are irregular with sizes comprised in the 1–10 μm range. A completely different morphology is generated by phase separation along the cloud-point curve, i.e. curing at $T_i = 230°C$ (*Figures 4b* and *4c*). Now, a random distribution of spherical particles is clearly evidenced. Examination of fracture surfaces revealed the presence of bands of different roughness associated with different propagation rates. The particles were highly drawn during the slow step of crack propagation, through a crack bridging mechanism. Ductile particles, rich in PBT, bridge the crack faces and plastically draw[3,4] (the white central part of dispersed-phase particles shown in *Figures 4b* and *4c*, is the portion drawn to fracture in a direction perpendicular to the micrograph plane). Signs of crack path deflection and bifurcation lines[3], are also present in the micrographs.

The size distribution of dispersed phase particles, obtained from SEM micrographs, was the same for fracture surfaces and polished surfaces. This means that particle sizes do not vary during crack propagation, a fact that reflects that there is good adhesion to the matrix. Without this adhesion, the second phase could prematurely de-bond before deformation could occur[4].

Table 1 shows several parameters characterizing the morphologies generated when curing at $T_i = 230°C$. Increasing the PBT amount increases the average size but not the concentration of dispersed phase particles. The volume fraction of dispersed phase (V_D) increases in the same proportion than the initial PBT concentration, within experimental error. The initial volume fractions of PBT in both formulations were 0.035 and 0.070, calculated from the densities of every component[1], and assuming no volume change upon mixing. The experimental volume fractions of dispersed phase were 0.063 and 0.112, respectively. The following facts may explain this discrepancy: (i) there is a significant amount of epoxy–amine species segregated to the dispersed domains in the course of the phase separation process[5–7], and/or (ii) the experimental value of V_D arises from the plane of crack propagation which includes particles present in different planes of the initial sample[8].

Mechanical properties of the neat matrix and PBT-modified materials with different morphologies are shown in *Table 2*. Material 1 is the neat matrix and materials 2–4 exhibit the morphologies shown in *Figures 4a–4c*, respectively. While the yield stress is constant within experimental error, a small but significant increase in K_{Ic} is produced by the presence of PBT particles. It lies in the same range that several values reported in the literature[3] when small amounts of a thermoplastic are used to modify epoxides exhibiting high glass transition temperatures (T_gs). The absence of plastic deformation in the high-T_g epoxy matrix is the main cause of the small increase of the K_{Ic} value which is almost exclusively derived from the plastic deformation of the thermoplastic second phase.

Table 1 Particle concentration (N), average diameter ($\bar{D}$) and volume fraction of dispersed phase (V_D), for PBT–DGEBA–DDS materials containing different wt% PBT and cured at 230°C

wt% PBT	N (part μm^{-2})	$\bar{D}$ (μm)	V_D
3.75	0.13	0.76	0.063
7.5	0.12	1.06	0.112

Table 2 Yield stress (σ_y) and critical stress intensity factor (K_{Ic}) of the neat DGEBA–DDS matrix and PBT–DGEBA–DDS materials, cured using different thermal cycles

Material	wt% PBT	Thermal cycle	σ_y (MPa)	K_{Ic} (MPa $m^{1/2}$ ± 0.05)
1	0	2 h 180°C + 2 h 230°C	121	0.70
2	3.75	2 h 180°C + 2 h 230°C	119	0.80
3	3.75	15′ 230°C + 3.5 h 200°C	119	0.90
4	7.5	15′ 230°C + 3.5 h 200°C	120	0.80

The generation of a distribution of semicrystalline particles with sizes in the 1 μm range (materials 3 and 4), through phase separation in the course of reaction, did not produce a significant increase in K_{Ic} value over the one obtained when larger-size irregular domains were produced by crystallization before reaction (material 2). The small ΔK_{Ic} values observed in this study, suggest that phase transformation toughening by PBT particles, does not occur or is not as efficient as previously reported[9].

After post-curing during 3 h at $T_i = 230°C$, PBT-modified materials exhibited T_g values close to that of the neat matrix, i.e. $T_g = 210–214°C$. This means that PBT was practically exhausted from the matrix in PBT–DGEBA–DDS formulations. This was not the case when DDS was replaced by MCDEA as will be discussed in the next section.

PBT–DGEBA–MCDEA systems

As discussed in the first part of the series[1], no cloud-point curve is present in the CTT diagram of a PBT-modified DGEBA-MCDEA formulation. Therefore, if the cure is produced at temperatures high enough to avoid PBT crystallization, i.e. $T_i \geq 210°C$, homogeneous materials are obtained. The following describes this particular case.

A DGEBA–MCDEA formulation containing 3.3 wt% PBT was cured at $T_i = 210°C$ during 3.5 h, in order to assure full conversion. A similar thermal cycle was used to cure the neat matrix. After a slow cooling to room temperature both materials were transparent. The absence of a dispersed phase in the PBT-modified material was verified by examination of SEM micrographs of fracture surfaces. Obviously, the possibility of phase separation at a smaller scale cannot be excluded.

Dynamic mechanical thermal analysis showed that the α-relaxation (maximum in $\tan\delta$), decreased from 179°C for the pure matrix to 168°C for the material modified with 3.3 wt% PBT. Therefore, the PBT remaining dissolved in the matrix introduces plasticization. The decrease in T_g may be predicted using a conventional rule-of-mixtures law, such as Fox's equation[10]:

$$1/T_g = w(\text{PBT})/T_g(\text{PBT}) + [1 - w(\text{PBT})]/T_g(\text{matrix}) \quad (7)$$

where $w(\text{PBT}) = 0.033$ is the mass fraction of PBT and $T_g(\text{matrix}) = 452\,K$ (179°C). It has been shown[11], that PBT has an unusual behaviour with two, well separated glass transitions. The first, at 248 K, is characteristic of amorphous PBT and is normally absent in semicrystalline samples. The second, at about 310–315 K, is characteristic of a 'rigid amorphous state' which is the usual state in semicrystalline samples[11]. Then, using $T_g(\text{PBT}) =$ 248 K in equation (7), leads to $T_g = 167°C$, in good agreement with the experimental value (168°C).

The elastic modulus (E) and the critical stress intensity factor (K_{Ic}) of both materials, are shown in *Table 3*. It is observed that the dissolution of PBT in the matrix did not introduce any toughening effect (the slight decrease observed in K_{Ic} is comprised within the experimental error). Phase separation is a necessary condition to generate new mechanisms increasing the resistance to crack propagation. Therefore, for a PBT–DGEBA–MCDEA system the generation of a dispersed phase requires: (i) to crystallize PBT before reaction, (ii) to keep $T_i < T_m$ at least up to the gel conversion (preferably during the whole thermal cycle to avoid partial dissolution of amorphous PBT).

Table 3 Elastic modulus (E) and critical stress intensity factor (K_{Ic}) of the neat DGEBA–MCDEA matrix and PBT–DGEBA–MCDEA containing 3.3 wt% PBT (homogeneous material with PBT remaining in solution)

wt% PBT	E (GPa)	K_{Ic} (MPa m$^{1/2}$ ± 0.05)
0	2.4	0.60
3.3	2.4	0.55

CONCLUSIONS

Different morphologies and associated thermal and mechanical properties could be obtained in epoxies modified by a small amount of a semicrystalline thermoplastic. Depending on the nature of the initial system, the cure at $T_i > T_m$ led to the absence of phase separation (DGEBA–MCDEA), or to the generation of a random dispersion of spherical particles rich in modifier (DGEBA–DDS). In the first case, no crystallization was observed when cooling to room temperature; in the last case, crystallization of the modifier inside dispersed domains took place during the cooling step. SAXS and WAXS, carried out *in situ* during reaction, showed that the generation of a random distribution of dispersed phase particles was an earlier event than the crystallization occurring inside dispersed domains.

The generation of a second phase rich in modifier is a necessary condition to introduce a toughening effect (even if it was a modest one in the present study). Crack bridging by highly drawn thermoplastic particles is the main mechanism increasing the fracture resistance to crack propagation. For the particular concentration range explored in the present study, no significant differences in K_{Ic} values were found when the modifier was present as a broad distribution of irregular-shape crystals (produced by crystallization before reaction), or as a narrow distribution of small spherical particles (produced by reaction-induced phase separation).

ACKNOWLEDGEMENTS

This work was conducted in the frame of a cooperation agreement between CONICET (Argentina) and CNRS (France), as well as an international cooperation program of Fundación Antorchas (Argentina).

REFERENCES

1 Oyanguren, P. A., Frontini, P. M., Williams, R. J. J., Girard-Reydet, E. and Pascault, J. P. *Polymer*, 1996, **37**, 3079
2 Chen, D., Pascault, J. P., Sautereau, H. and Vigier, G. *Polym. Int.* 1993, **32**, 369
3 Pearson, R. A. in 'Toughened Plastics I: Science and Engineering' (Eds C. K. Riew and A. J. Kinloch), Adv. Chem. Ser. no 233, American Chemical Society, Washington DC, 1993, p. 405
4 Cardwell, B. J. and Yee, A. F. *Polym. Mat. Sci. Eng. (ACS)* 1994, **70**, 254

5 Williams, R. J. J., Borrajo, J., Adabbo, H. E. and Rojas, A. J. in 'Rubber-Modified Thermoset Resins' (Eds C. K. Riew and J. K. Gillham), Adv. Chem. Ser. no 208, American Chemical Society, Washington DC, 1984, p. 195
6 Verchère, D., Sautereau, H., Pascault, J. P., Moschiar, S. M., Riccardi, C. C. and Williams, R. J. J. in 'Toughened Plastics I: Science and Engineering' (Eds C. K. Riew and A. J. Kinloch), Adv. Chem. Ser. no 233, American Chemical Society, Washington DC, 1993, p. 335
7 Riccardi, C. C., Borrajo, J. and Williams, R. J. J. *Polymer* 1994, **35,** 5541
8 Verchère, D., Pascault, J. P., Sautereau, H., Moschiar, S. M., Riccardi, C. C. and Williams, R. J. J. *J. Appl. Polym. Sci.* 1991, **42,** 701
9 Kim, J. and Robertson, R. E. *J. Mater. Sci.* 1992, **27,** 3000
10 Fox, T. G. *Bull. Am. Phys. Soc.* 1956, **1,** 123
11 Cheng, S. Z. D., Pan, R. and Wunderlich, B. *Makromol. Chem.* 1988, **189,** 2443